J Therm Anal Calorim (2012) 110:249–256
DOI 10.1007/s10973-012-2362-y

The kinetic and thermodynamic study of $KNiPO_4 \cdot H_2O$ from DSC and TG data

Chanaiporn Danvirutai · Pittayagorn Noisong · Tipaporn Srithanrattana

CEEC-TAC1 Conference Special Issue

Abstract The DSC and TG data showed the dehydration process occurring over the range of 160–300 °C. The XRD patterns of the synthesized $KNiPO_4 \cdot H_2O$ and the calcined product at 350 °C with exposing in the air over 8 h are indexed as the $KNiPO_4 \cdot H_2O$ structure, whereas at 600 °C is indexed as $KNiPO_4$ structure. Hence, these data confirmed that the water molecule was eliminated from the structure at 300 °C, after that the spontaneously reversible hydration–rehydration process was observed. The activation energy and pre-exponential factor were calculated by Kissinger, Ozawa, and KAS equations. According to the DSC curves, the enthalpy change (ΔH) of dehydration process can be calculated and was found to be 100.12 kJ mol^{-1}. Besides, we suggested another new method to determine the isokinetic temperature value using spectroscopic data. The surface area of synthesized hydrate and its calcined product at 350 °C with exposing in the air at over 8 h were found to be 21.48 and 134.3 $m^2\ g^{-1}$, respectively. The reversible hydration–rehydration process was observed, and the surface area of final product at 350 °C (aging time over 8 h) is higher than that of the synthesized compound. This behavior is important to develop alternative desiccant materials or other process based on the rehydration mechanism with increasing the surface area.

Keywords $KNiPO_4 \cdot H_2O$ · Kinetics · Reversible reaction · Thermodynamics

C. Danvirutai (✉) · P. Noisong · T. Srithanrattana
Department of Chemistry, Faculty of Science, Khon Kaen University, Khon Kaen 40002, Thailand
e-mail: chanai@kku.ac.th

C. Danvirutai · P. Noisong
Department of Chemistry and Center of Excellence for Innovation in Chemistry, Faculty of Science, Khon Kaen University, Khon Kaen 40002, Thailand

C. Danvirutai
Advanced Functional Materials Research Cluster, Khon Kaen University, Khon Kaen, Thailand

Introduction

The metal phosphate of dittmarite series $M^IM^{II}PO_4 \cdot H_2O$ ($M^I = K^+$, NH_4^+, $M^{II} = Mn^{2+}$, Mg^{2+} Fe^{2+}, Co^{2+}, Ni^{2+}, Zn^{2+}) is a biomineral found in urinary calculi [1]. They have widely attracted due to their potential to form framework structures (having a layer structure with metal(II) phosphate sheets separated by K^+ or NH_4^+ ions) [2] and can be applied as complex fertilizers [3–6] containing three nutrient elements: the corresponding mono valence cation (nitrogen or potassium), phosphorus, and the corresponding metal (magnesium, iron, manganese, zinc, cobalt, nickel, copper, etc.). Some of them are used as pigments in artist's paints [6, 7] and to extract cations from sea water [6]. In the fact, the atomic sizes of divalent cation Mn, Fe, Ni, and Co are very close to each other. Therefore, the mixed metal in these series can be generated, such as $NH_4Mn_{0.5}Fe_{0.5}PO_4 \cdot H_2O$, $NH_4Ni_{0.5}Co_{0.5}PO_4 \cdot H_2O$, $KMn_{0.5}Fe_{0.5}PO_4 \cdot H_2O$, and $KNi_{0.5}Co_{0.5}PO_4 \cdot H_2O$. The resulted compounds can improve the efficiency for an extraction of bivalent cations from sea water. Therefore, these compounds are attracted for studying the simple synthetic route and the physical as well as chemical properties. Despite the vibrational behavior of dittmarite series was widely studied in the literature [8–10], unfortunately, the thermal analysis of this series has received little attention. Recently, the thermal analysis (TG/DTG/DTA and DSC) methods have

been widely used for scientific and practical purposes [11–16]. The results obtained from these methods can be directly applied in materials science for the preparation of various metal alloys, cements, ceramics, glasses, enamels, glazes, polymer, and composite materials [11]. Non-isothermal methods are becoming more widely used because they are more convenient than the classical isothermal methods. In our previous papers [17–19], the kinetic and thermodynamic properties of manganese hypophosphite compound, $KMnPO_4{\cdot}H_2O$ and $NH_4MnPO_4{\cdot}H_2O$, were studied by non-isothermal method using various equations. In this respect, they are of great interest to be selected for studying their kinetic and thermodynamic properties of thermal decomposition. A part from that, the kinetic compensation effect (KCE) describes a linear relationship between the activation energy (E) and the logarithm of the pre-exponential factor ($\ln A$) with the following equation will be considered:

$$\ln A = aE + b \tag{1}$$

where a and b are the kinetic compensation constant values and the isokinetic temperature (T_i) calculated from the equation,

$$T_i = 1/a\,R \tag{2}$$

where R is a gas constant (8.314 J K^{-1} mol^{-1}). The authors demonstrated [20] based on the equation suggested by Vlase et al. [21] that the specificity of non-isothermal decomposi tion is due to the vibrational energy on a certain bond, which based on anharmonic oscillation. Consequently, the wave number of the activated bond can be calculated from the isokinetic temperature T_i using [20, 21]:

$$\omega_{\text{calc}} = \frac{k_B}{hc} T_i = 0.695\ T_i \tag{3}$$

and

$$\omega_{\text{sp}} = q\omega_{\text{calc}} \tag{4}$$

$$\omega_{\text{calc}} = \omega_{\text{sp}}/q \tag{5}$$

where k_B and h are the Boltzmann and Planck constants, respectively, c is the light velocity, q is the number of quanta ($q \in N$), and ω_{sp} is the assigned spectroscopic wavenumber for the bond supposed to be broken. T_i is the isokinetic temperature as related to the activation energy and preexponetial factor [22–24]. The calculation of this value is complicated; therefore, the calculation of isokinetic temperature T_i is suggested to be calculated from spectroscopic data as an alternative way.

The aims of this work are to present the study of kinetic properties of $KNiPO_4{\cdot}H_2O$ from DSC data using the Kissinger method. In addition, the new procedure to determine the isokinetic temperature value from spectroscopic data is suggested. The enthalpy of the dehydration (ΔH) of the title compound can be calculated for the first time.

Experimental

Preparation and characterization

The $KNiPO_4{\cdot}H_2O$ was synthesized according to the Basset and Bedwell [25] methods. In typical synthesis, 20 mL of 0.5 M nickel chloride hexahydrate ($NiCl_2{\cdot}6H_2O$, Ajax Finechem Pty Ltd.) was added by 60 mL of saturated dipotassium hydrogen phosphate ((K_2HPO_4), 99%, Carlo erba) and digested at 85 ± 5 °C for 3 days. After that the pale green precipitation was obtained followed by filtered and washed by DI water and kept in the desiccator. The metal and water contents of the synthesized hydrates were confirmed using atomic absorption spectrophotometry (AAS, Perkin Elmer, Analyst 100) and TG/DTG/DTA (Perkin-Elmer, Pyris Diamond). Differential scanning calorimetry (DSC, Perkin Elmer, Pyris One) was carried out using ca 5.0–10.0 mg (accurate) of sample in an aluminum crucible. The curves of both TG/DTG/DTA and DSC were recorded over the temperature range of 60–500 °C with four heating rates of 10, 15, 20, and 25 °C min^{-1}. The dehydration and the thermal transformation products obtained from the calcinations in air atmosphere were further characterized. The FTIR spectra of the synthesized compound and its calcined samples were recorded in the range of 4,000–370 cm^{-1} using KBr pellet technique (KBr, Merck, spectroscopy grade) on a Perkin Elmer spectrum GX FTIR/FT Raman spectrophotometer with eight scans and the resolution of 4 cm^{-1}.

The structures of the prepared hydrate and its calcined products were characterized using XRD (D8 Advanced powder diffractometer, Bruker AXS, Karlsruhe, Germany) with Cu K_α radiation ($\lambda = 0.15406$ Å). The Scherrer method was used to evaluate the crystallite sizes (i.e., $D = K\lambda/\beta\cos\theta$, where λ is the wavelength of X-ray radiation, K is a constant taken as 0.89, θ is the diffraction angle and β is the full width at half maximum (FWHM)). [26].

Kinetics studies

The kinetics of thermal decomposition reaction can be described by various equations taking into account the special features of their mechanisms. The kinetic treatment of the non-isothermal decomposition for the dehydration of crystalline hydrates is considered as solid-state process of the type: A (solid) → B (solid) + C (gas) [27–30]. The solutions of kinetic equations have been reported in the literatures [31–35]. The kinetic analyses can be carried out by various methods such as Kissinger [36], Ozawa [37], Kissiger–Akahira and Sunose (KAS) [38], Coats–Redfern [39], Van Krevelens [40], etc. The model-free or isoconversional method involves measuring temperatures corresponding to the fix value of extent of conversion (α) at

different heating rates (β). The interest in these methods (e.g., Kissinger, Ozawa, and KAS) has increased recently due to the ability to calculate the activation energy values without modelistic assumptions. In addition, the Kissinger method can be applied to calculate the pre-exponential factor, while the Ozawa and KAS methods can be used only to calculate the activation energy E values without modelistic appropriation. However, Ozawa and KAS methods can be used to determine the pre-exponential factor, if the mechanism process is known. The Kissinger equation (Eq. 6) is the simple determination of kinetic parameters (the activation energy (E) and pre-exponential factor (A)) and widely used in the literature [31, 41]. In addition, Ozawa [37] and KAS [38] equations are model-free method that is also well described and widely used in the literatures. Therefore, these equations are selected for the kinetic analysis of the dehydration for the studied compound.

Kissinger equation:

$$\ln\left[\frac{\beta}{T_P^2}\right] = \ln\left[\frac{AR}{E}\right] - \frac{E_a}{RT_P} \tag{6}$$

Ozawa equation:

$$\ln\beta = \ln\left(\frac{0.0048AE}{g(\alpha)R}\right) - 1.0516\left(\frac{E}{RT}\right) \tag{7}$$

KAS equation:

$$\ln\frac{\beta}{T^2} = \ln\frac{AR}{g(\alpha)E} - \frac{E}{RT} \tag{8}$$

where A is the pre-exponential factor (min^{-1}) and is assumed to be independent of temperature, α is the extent of conversion, $g(\alpha)$ is a kinetic function depending on the reaction mechanism and is referred to as the integral form, E is the activation energy (kJ mol^{-1}), β is the heating rate (°C min^{-1}), and R is the gas constant. According to the above-mentioned equations, the plots of $\ln\left(\beta/T_p^2\right)$ versus $1000/T_p$ (Eq. 6), $\ln\beta$ versus $1000/T$ (Eq. 7), and $\ln(\beta/T^2)$ versus $1000/T$ (Eq. 8) can be obtained by a linear regression of least-square method. The activation energies E and pre-exponential factor A can be evaluated from the slopes and interceptions of the straight lines with better linear correlation coefficient (R^2), respectively.

Results and discussion

TG/DTG/DTA and DSC

The TG/DTG/DTA curves of studied compounds are presented in Fig. 1. This compound is stable in the range of temperature below 160 °C. The percentage of mass loss is

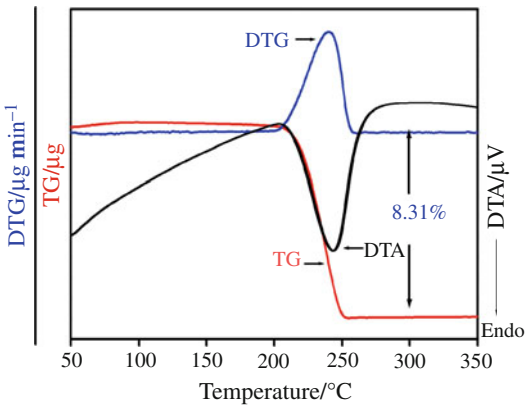

Fig. 1 TG/DTG/DTA curves of the synthesized $KNiPO_4 \cdot H_2O$ at the heating rate of 10 °C min^{-1} in air atmosphere

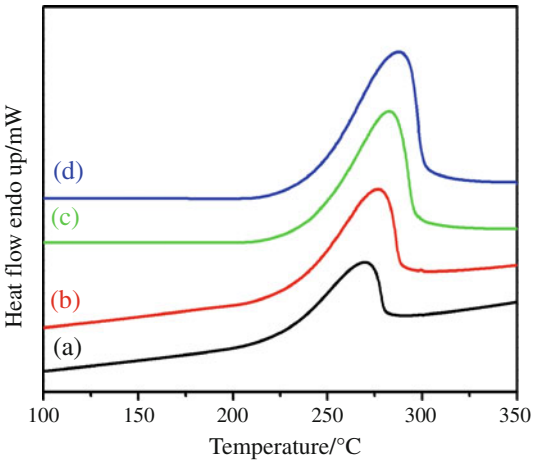

Fig. 2 DSC curves of the synthesized $KNiPO_4 \cdot H_2O$ at the heating rates of (*a*) 10, (*b*) 15, (*c*) 20, and (*d*) 25 °C min^{-1}

8.31% which corresponds to 0.97 mol of water. The dehydration process starts at about 160 °C and finished at about 300 °C (maximum temperature peak is 233.40 °C). The DSC curves of the studied compound were recorded at the four heating rates of 10, 15, 20, and 25 °C min^{-1} and presented in Fig. 2. The endothermic peak was observed in the DSC curve of $KNiPO_4 \cdot H_2O$ for the heating rate of 10 °C min^{-1} (Fig. 2a), which corresponds to the dehydration process. The DSC curve shows the single peak which is in good agreement with DTG and DTA curves as shown in Fig. 1.

FTIR spectra

The FTIR spectra of the title compound and its thermal decomposition products at 350 °C (aging time over 8 h) and 600 °C in air atmosphere are presented in Fig. 3a–c, respectively. The FTIR spectrum of the studied compound

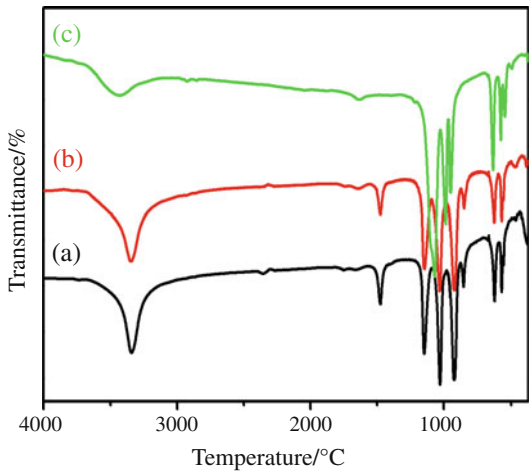

Fig. 3 FTIR spectra of the synthesized $KNiPO_4{\cdot}H_2O$ (*a*), its calcined product at 350 °C (aging time over 8 h) (*b*), and its calcined product at 600 °C (*c*) in air atmosphere

is similar to its calcined product at 350 °C (aging time in the air over 8 h). The band at 3,343 cm^{-1} in Fig. 3a and b is assigned to O–H stretching vibration ($v_1(H_2O)$), and the band at 1,651 and 1,477 cm^{-1} is assigned to the bending and very low bending ($v_2(H_2O)$) of water molecule, while the strong bands in the range of 1,145–917 cm^{-1} and the two bands in the range of 620–565 cm^{-1} are assigned to the P–O stretching or $v_3(F_2)$ and OPO bending or $v_4(F_2)$ vibrations of PO_4^{3-} anion, respectively. The identification of the decomposition products at each calcined temperature was supported by the results from FTIR spectra. Figure 3b confirmed that the water molecule was eliminated from the structure at 350 °C, after that the rehydration process occurred when exposed to the air. Figure 3c illustrates that the P–O stretching or $v_3(F_2)$ mode of $[PO_4]^{3-}$ anion is known to appear in the 1,100–950 cm^{-1} region [2, 8]. The calcined product at 600 °C (Fig. 3c) exhibits the same characteristic as that of $KNiPO_4$. The detail of vibrational wavenumbers was explained by comparing with those observed in our previous work and reference [10, 19]. Therefore, the mechanism of mass loss and the rehydration process can be suggested as the following:

$$KNiPO_4 \cdot H_2O(s) \rightleftharpoons H_2O\ (g) + KNiPO_4(s) \quad (9)$$

This study presents the method to determine isokinetic temperature value from spectroscopic data. The observed vibrational energy in terms of ω_{sp} of water molecule in the water of crystallization molecules appear in three positions: 3,343, 1,651, and 1,477 cm^{-1} (Fig. 3a). Therefore, the calculated wavenumber (ω_{calc}) values were obtained using Eq. 5 for different number of quanta (q) and the ω_{sp} values are presented in Table 1. We selected the ω_{calc} values those that are closest to three vibrational FTIR band positions according to the vibrational energy of the same molecule. These data reveal that the quanta numbers of the O–H stretching, bending, and very low bending of water of crystallization molecule are 10, 5, and 4, respectively. The average ω_{calc} value and calculated T_i from Eq. 3 are tabulated in Table 1, which illustrate the new method of isokinetic temperature calculation from spectroscopic data.

X-ray powder diffraction

The XRD patterns of the synthesized $KNiPO_4{\cdot}H_2O$ and its calcined products at 350 °C with exposing in the air over 8 h and 600 °C in air atmosphere are shown in Fig. 4. All detectable peaks of the $KNiPO_4{\cdot}H_2O$ and the calcined

Table 1 Calculated isokinetic temperature (T_i) from spectroscopic data and KCEs study

ω_{sp}/cm^{-1} Observed in FTIR spectra	q	ω_{calc}/cm^{-1}	Assignment	The selected ω_{calc}/cm^{-1}	Average ω_{calc}/cm^{-1}	T_i/K	T_i/K	
							KCEs study	
							Ozawa	KAS
3,343	2	1,672	O–H stretching of water of crystallization molecules	334				
	4	836						
	6	557						
	8	418						
	10	334						
1,651	1	1,651	H–O–H bending of water of crystallization molecules	330	344.33	495.44	481.56	475.39
	3	550						
	5	330						
	7	236						
1,477	2	738	H–O–H very low bending of water of crystallization molecules	369				
	4	369						
	6	246						
	8	184						

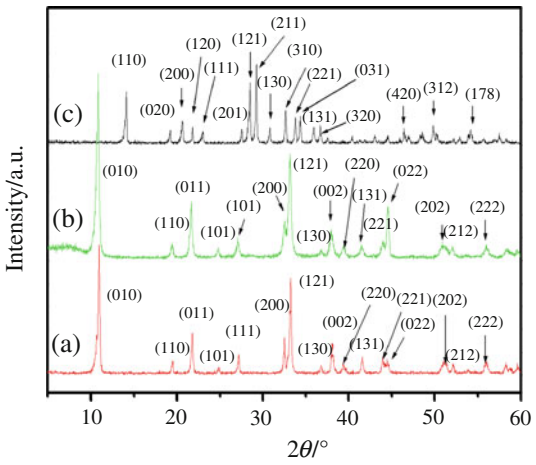

Fig. 4 XRD patterns of the synthesized (*a*) $KNiPO_4 \cdot H_2O$, (*b*) the calcined product at 350 °C (aging time over 8 h), and (*c*) 600 °C in air atmosphere

product at 350 °C exposing in the air are indexed as the synthesized $KNiPO_4 \cdot H_2O$ structure (PDF #860593), whereas the calcined product at 600 °C is indexed as $KNiPO_4$ structure (PDF #860573). The results indicate that both $KNiPO_4 \cdot H_2O$ and $KNiPO_4$ crystallize in an orthorhombic crystal system with the space group $Pmn2_1$ (C_{2v}^7) and $Pna2_1$ (C_{2v}^9), respectively. The lattice parameters of the synthesized compound and its calcined products are compared with those reported in the standard data and found to agree well as presented in Table 2. The results confirmed the reversible hydration–rehydration process in the studied compound. This behavior can be applied for the development of alternative desiccant materials or other processes related to the rehydration mechanism.

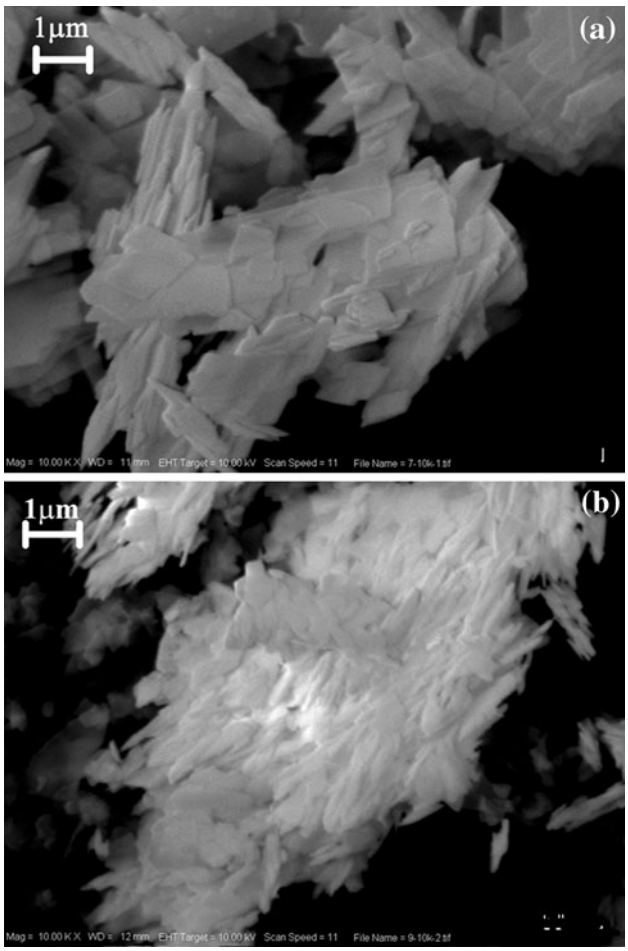

Fig. 5 SEM micrographs of the synthesized $KNiPO_4 \cdot H_2O$ (**a**) and its calcined product at 350 °C (aging time over 8 h) (**b**)

SEM and BET

The SEM micrographs of the $KNiPO_4 \cdot H_2O$ and its calcined product at 350 °C (aging time over 8 h) are shown in Fig. 5. The SEM micrograph of $KNiPO_4 \cdot H_2O$ (Fig. 5a) illustrates the thin plated coalescence and irregular plates. Whereas, its calcined product at 350 °C (aging time over 8 h) shows the agglomeration of sheet and the morphologies with smaller size than that of $KNiPO_4 \cdot H_2O$. The surface area of synthesized hydrate and its final product at

Table 2 Average particle sizes and lattice parameters of $KNiPO_4 \cdot H_2O$ and its calcined products at 350 (aging time over 8 h) and 600 °C in air atmosphere calculated from XRD data

Compound	Method	*a*/Å	*b*/Å	*c*/Å	Average particle sizes/nm
$KNiPO_4 \cdot H_2O$	PDF#860593	5.537	8.216	4.744	44.80 ± 16
	This work	5.564	8.197	4.730	
	DIF. PDF-this work	−0.027	0.019	0.014	
$KNiPO_4 \cdot H_2O$ ($KNiPO_4 \cdot H_2O$ calcined at 350 °C)	PDF#860593	5.537	8.216	4.744	37.83 ± 10
	This work	5.515	8.158	4.714	
	DIF. PDF-this work	0.022	0.058	0.030	
$KNiPO_4$	PDF#860573	8.633	9.256	4.906	84.42 ± 19
	This work	8.804	9.594	4.937	
	DIF. PDF-this work	−0.171	−0.238	−0.031	

350 °C with exposing in the air at over 8 h were measured by nitrogen adsorption according to Brunaner, Emmett, and Teller (BET) method and found to be 21.48 and 134.3 $m^2\ g^{-1}$, respectively. It was found that the surface area of final product at 350 °C (aging time over 8 h) followed by rehydration of the new rehydration product is higher than that of the starting synthesized compound.

Kinetic and thermodynamic studies from DSC data

The maximum peak temperature of DSC curves at various heating rates was used to determine the activation energy (E) and pre-exponential factor (A) using Kissinger equation, and the results are presented in Table 3. According to the DSC curves at the four heating rates of 10, 15, 20, and 25 °C min^{-1}, the enthalpy changes (ΔH) of dehydration process can be calculated and were found to be 476.913 J g^{-1} (100.53 kJ mol^{-1}), 482.836 J g^{-1} (101.78 kJ mol^{-1}), 483.900 J g^{-1} (102.01 kJ mol^{-1}), and 456.230 J g^{-1} (96.17 kJ mol^{-1}), respectively. The mean of this value is 100.12 ± 2.71 kJ mol^{-1}. The studied compound shows the reversible dehydration–rehydration process; therefore at the peak temperature (T_p), the Gibbs free energy (ΔG) change is 0 kJ mol^{-1}. The dehydration is endothermic (ΔH is positive) and reversible process (ΔG is zero).

The kinetic study from TG data

The calculated activation energy and pre-exponential factor from the Kissinger equation are 111.21 kJ mol^{-1} and 1.27×10^{11} min^{-1}, respectively. While the same parameters determined from Ozawa and KAS equations are presented in Table 4 and found to decrease slightly with the increasing of the extent of conversion function (α). The results in Table 4 reveal that the activation energy (E) is independent on the extent of conversion (α) which indicate the single step reaction. Thus, the following equation can be used to estimate the most probable reaction mechanism:

$$\ln g(\alpha) = \left[\ln \frac{AE}{R} + \ln \frac{e^{-x}}{x^2} + \ln h(x)\right] - \ln \beta \qquad (10)$$

where x is E/RT and $h(x)$ is expressed by the fourth Senum and Yang approximation as described in references [42] and [43]. The plots of $\ln(g(\alpha))$ versus $\ln(\beta)$ can be carried out using a linear regression of least square method. To determine the most probable mechanism function, the degree of conversion α corresponding to four heating rates taken at the same temperature (we selected at maximum temperature in each decomposition process) was substituted into the left-hand side of Eq. 10 for all 26 types of mechanism functions as presented in the literature

Table 3 The maximum peak temperatures at four heating rates, the activation energy (E), pre-exponential factor (A), and correlation coefficient (R^2) calculated from DSC and TG data

β/°C min^{-1}	T_p/K DSC/TG	E/kJ mol^{-1} DSC/TG	A/min^{-1} DSC/TG	R^2 DSC/TG
10	542.06/510.16	114.24/111.21	4.90×10^{10}/1.27×10^{11}	0.9936/0.9979
15	548.88/516.91			
20	555.51/522.7			
25	560.66/527.19			

Table 4 Activation energy values (E), pre-exponential factor (A), and correlation coefficient (R^2) calculated by Ozawa and KAS methods for the dehydration process of $KNiPO_4{\cdot}H_2O$ in N_2 atmosphere from TG data

A	Ozawa			KAS		
	E/kJ mol^{-1}	R^2	A	E/kJ mol^{-1}	R^2	A/min^{-1}
0.2	139.16 ± 13.91	0.9804	6.68×10^{14}	138.45 ± 14.64	0.9781	7.78×10^{14}
0.3	132.02 ± 11.75	0.9844	1.45×10^{14}	130.86 ± 12.37	0.9824	1.02×10^{14}
0.4	125.46 ± 10.06	0.9873	2.62×10^{13}	123.90 ± 10.61	0.9855	1.64×10^{13}
0.5	122.99 ± 10.48	0.9857	1.36×10^{13}	121.24 ± 11.04	0.9837	8.03×10^{12}
0.6	120.87 ± 10.70	0.9846	7.81×10^{12}	118.96 ± 11.27	0.9994	4.39×10^{12}
0.7	117.30 ± 9.18	0.9879	3.18×10^{12}	115.15 ± 9.68	0.9823	1.66×10^{12}
0.8	116.05 ± 9.05	0.9880	2.34×10^{12}	113.79 ± 9.54	0.9861	1.18×10^{12}
Average	124.84 ± 9.39	0.9855	1.67×10^{14}	123.19 ± 11.31	0.9835	1.30×10^{14}

Table 5 The most probable mechanism functions $g(\alpha)$, slopes, and the correlation coefficients of linear regression (R^2) calculated from Eq. 10 for $KNiPO_4 \cdot H_2O$

Step	Temperature/°C	Mechanism No.	R^2	Slope
Step 1	210	$F_{1/3}$	**0.9834**	**−1.05779**
		$F_{3/4}$	0.9879	−1.18932
		A_1	0.9902	−1.2740
		$A_{3/2}$	**0.9902**	**−0.84933**
		A_2	0.9902	−0.6370
		R_2, $F_{1/2}$	0.9853	−1.10897
		D_5	0.9928	−2.7873
	220	$F_{1/3}$	**0.9756**	**−0.90751**
		$F_{3/4}$	0.9910	−1.23543
		A_1	0.9962	−1.47578
		$A_{3/2}$	**0.9962**	**−0.98386**
		A_2	0.9962	−0.73789
		R_2, $F_{1/2}$	0.9828	−1.02818
		D_5	0.9994	−3.69751

[19]. If the mechanism function g(α) according to Eq. 10 exhibits the slope and the linear correlation coefficient R^2 closest to −1.0000 and unity, respectively, then the function $g(\alpha)$ is the most probable mechanism function. After that the pre-exponential factor can be evaluated from the interceptions in Eqs. 7 and 8. The calculated results from Eq. 10 are presented in Table 5. Consequently, it can be stated that the most probable mechanism function with the integral form $g(\alpha) = 1 - (1 - \alpha)^{2/3}$ and differential form $f(\alpha) = 3/2(1 - \alpha)^{1/3}$ belong to the mechanism of one-third order reaction ($F_{1/3}$) [33]. The rate law equation based on calculated kinetic data from KAS method can be suggested to be as following:

$$1 - (1 - \alpha)^{2/3} = 1.30 \times 10^{14} e^{-123.19/RT} \quad (11)$$

The isokinetic temperature T_i was calculated through the KCEs method and found to be close to the calculated one from the spectroscopic data (Table 1). Therefore, this procedure can be an alternative method to calculate the isokinetic temperature.

Conclusions

The dehydration of $KNiPO_4 \cdot H_2O$ occurs over the temperature range 160–300 °C without destruction of the layered structure, which was confirmed by its decomposition product at 350 °C (aging time on the air is over 8 h) exhibiting the spontaneous rehydration process to form the same compound as the initial one. This phenomenon can be confirmed by FTIR and XRD measurements. In addition, the surface area of the reversible hydration product is higher than that of the initial synthesized one. This finding is important to the development of alternative desiccant materials as well as the catalysts of high-surface area or other processes based on the rehydration mechanism. This study suggests the new procedure to determine the isokinetic temperature value from spectroscopic data, instead of the complicated relationship between activation energy and pre-exponential factor. The average enthalpy change of this process was found to be 100.12 kJ mol^{-1}, whereas the Gibbs-free energy change was assumed to be 0 kJ mol^{-1} according to the reversible process in the studied compound. The activation energy and pre-exponential factor of dehydration process were calculated from Kissinger equation using both TG/DTG/DTA and DSC data. The results found to agree well with each other. In addition, the activation energy values were calculated by Ozawa and KAS methods from TG/DTG/DTA data and found to confirm of single step dehydration. The calculated activation energy values from three methods are not significantly different.

This study reports the mean enthalpy change (ΔH) of dehydration of studied compound from the DSC measurements for the first time.

Acknowledgements We thank the Department of Chemistry, Faculty of Science, and Department of Environmental Engineering, Faculty of Engineering (for XRD) of Khon Kaen University for providing research facilities. The financial support from the Development and Promotion in Science and Technology Talents Project (DPST) and the Center of Excellence for Innovation Chemistry (PERCH-CIC), Commission on Higher Education, Ministry of Education through the Advanced Functional Materials Research Cluster, National Research University Project, Khon Kaen University is gratefully acknowledged.

References

1. Dao NQ, Daudon M. Infrared and Raman spectra of calculi. Paris: Elsevier; 1997.
2. Koleva VG. Metal–water interactions and hydrogen bonding in dittmarite-type compounds $M'M''PO_4 \cdot H_2O$ ($M' = K^+$, NH_4^+; $M'' = Mn^{2+}$, Co^{2+}, Ni^{2+}): correlations of IR spectroscopic and structural data. Spectrochim Acta. 2005;62:1196–202.
3. Yuan A, Wu J, Bai L, Ma S, Huang Z, Tong Z. Standard molar enthalpies of formation for ammonium/3d-transition metal phosphates $NH_4MPO_4 \cdot H_2O$ ($M = Mn^{2+}$, Co^{2+}, Ni^{2+}, Cu^{2+}). J Chem Eng Data. 2008;53:1066–70.
4. Ramajo B, Espina A, Barros N, Garćia JR. Thermal and thermo-oxidative decomposition of ammonium-iron(II) phosphate monohydrate. Thermochim Acta. 2009;487:60–4.
5. Salutsky ML, Steiger RP. Properties of fertilizer materials, metal potassium phosphates. J Agric Food Chem. 1964;12:486–91.
6. Lapina LM. Metal ammonium phosphates and their new applications. Russ Chem Rev. 1968;37:693–701.
7. Erskine AM, Grimm G, Horning SC. Ammonium ferrous phosphate, a pigment for metal protective paint finishes. Ind Eng Chem. 1944;36:456–60.
8. Šoptrajanov B, Stefov V, Kuzmanovski I, Jovanovski G, Lutz HD, Engelen B. Very low H-O-H bending frequencies. IV.

Fourier transform infrared spectra of synthetic dittmarite. J Mol Struct. 2002;613:7–14.
9. Šoptrajanov B, Jovanovski G, Pejov L. Very low H-O–H bending frequencies. III. Fourier transform infrared study of cobalt potassium phosphate monohydrate and manganese potassium phosphate monohydrate. J Mol Struct. 2002;613:47–54.
10. Šoptrajanov B. Very low H-O–H bending frequencies. I. Overview and infrared spectra of $NiKPO_4 \cdot H_2O$ and its deuterated analogues. J Mol Struct. 2000;555:21–30.
11. Vlaev L, Nedelchev N, Gyurova K, Zagorcheva M. A Comparative study of non-isothermal kinetics of decomposition of calcium oxalate monohydrate. J Anal Appl Pyrol. 2008;81:253–62.
12. Wendland WW. Thermal methods of analysis. New York: Wiley; 1974.
13. Šesták J. Thermophysical properties of solids. Prague: Academia; 1984.
14. Xu G, Fang B, Sun G. Kinetic study of decomposition of wheat distiller grains and steam gasification of the corresponding pyrolysis char. J Therm Anal Calorim. 2011;108:109–17.
15. Skreiberg A, Skreiberg ∅, Sandquist J, S∅rum L. TGA and macro-TGA characterisation of biomass fuels and fuel mixtures. Fuel. 2011;90:2182–97.
16. Al-Hajji LA, Hasan MA, Zaki MI. Kinetics of formation of barium tungstate in equimolar powder mixture of $BaCO_3$ and WO_3. J Therm Anal Calorim. 2010;100:43–9.
17. Noisong P, Danvirutai C, Boonchom B. Thermodynamic and kinetic properties of the formation of $Mn_2P_2O_7$ by thermal decomposition of $Mn(H_2PO_2)_2 \cdot H_2O$. J Chem Eng Data. 2009; 54:871–5.
18. Danvirutai C, Noisong P, Youngme S. Some thermodynamic functions and kinetics of thermal decomposition of $NH_4MnPO_4 \cdot H_2O$ in nitrogen atmosphere. J Therm Anal Calorim. 2009;100:117–24.
19. Noisong P, Danvirutai C. Kinetics and mechanism of thermal dehydration of $KMnPO_4 \cdot H_2O$ in a nitrogen atmosphere. Ind Eng Chem Res. 2010;49:3146–51.
20. Boonchom B, Danvirutai C. Thermal decomposition kinetics of $FePO_4 \cdot 3H_2O$ precursor to synthesize spherical nanoparticles $FePO_4$. Ind Eng Chem Res. 2007;46:9071–6.
21. Vlase T, Vlase G, Doca M, Doca N. Specificity of decomposition of solids in non-isothermal conditions. J Therm Anal Cal. 2003; 72:597–604.
22. Mianowski A, Marecka A. The isokinetic effect as related to the activation energy for the gases diffusion in coal at ambient temperatures, Part I. Fick's diffusion parameter estimated from kinetic curves. J Therm Anal Cal. 2009;95:285–92.
23. Ioitescu A, Vlase G, Vlase T, Doca N. Kinetics of decomposition of different acid calcium phosphates. J Therm Anal Cal. 2007; 88:121–5.
24. Pop N, Vlase G, Vlase T, Doca N, Mogos A, Ioitescu A. Compensation effect as a consequence of vibrational energy transfer in homogeneous and isotropic heat field. J Therm Anal Cal. 2008;92:313–7.
25. Basset H, Bedwell WL. Studies of phosphates. Part I. Ammonium magnesium phosphate and related compounds. J Chem Soc. 1933;137:854–71.
26. Cullity BD. Elements of X-ray diffraction. 2nd ed. New York: Addison-Wesley Publishing; 1978.
27. Vlaev LT, Nikolova MM, Gospodinov GG. Non-isothermal kinetics of dehydration of some selenite hexahydrates. J Solid State Chem. 2004;177:2663–9.
28. Vyazovkin S. A unified approach to kinetic processing of non-isothermal data. Int J Chem Kinet. 1996;28:95–101.
29. Vyazovkin S. Computational aspects of kinetic analysis. part C. The ICTAC kinetics project—the light at the end of the tunnel? Thermochim Acta. 2000;355:155–63.
30. Zhang KL, Hong JH, Cao GH, Zhan D, Tao YT, Cong CJ. The kinetics of thermal dehydration of copper(II) acetate monohydrate in air. Thermochim Acta. 2005;437:145–9.
31. Janković B, Kolar-Anić L, Smičiklas I, Dimović S, Aranđelović D. The non-isothermal thermogravimetric tests of animal bones combustion. Part I. Kinetic analysis. Thermochim Acta. 2009; 355:129–38.
32. Órfão JJM, Martins FG. Kinetic analysis of thermogravimetric data obtained under linear temperature programming—a method based on calculations of temperature integral by interpolation. Thermochim Acta. 2002;390:195–211.
33. Khawam A, Flanagan DR. Role of isoconversional methods in varying activation energies of solid-state kinetics II. Nonisothermal kinetic studies. Thermochim Acta. 2005;436:101–12.
34. Cai J, Liu R, Wang Y. Kinetic analysis of solid-state reactions: A new integral method for nonisothermal kinetic with the dependence of the preexponential factor on the temperature ($A = A_0T^n$). Solid State Sci. 2007;9:421–8.
35. Gao Z, Nakada M, Amasaki I. A consideration of errors and accuracy in the isoconversional methods. Thermochim Acta. 2001;369:137–42.
36. Kissinger HE. Reaction kinetics in differential thermal analysis. Anal Chem. 1957;29:1702–6.
37. Ozawa TA. New method of analyzing thermogravimetric data. Bull Chem Soc Jpn. 1965;38:1881–6.
38. Akahira T, Sunose T. Trans. 1969 joint convention of four electrical institutes, Paper No. 246. Res Report Chiba Inst Technol (Sci. Technol.). 1969; No.16, 22, 1971.
39. Coats AW, Redfern JP. Kinetic parameters from thermogravimetric data. Nature. 1964;20:68–9.
40. Van Krevelens DW, Hoftijzer PJ. Kinetics of gas−liquid reaction—general theory. Trans Ind Chem Eng. 1954;32:5360–83.
41. Pourmortazavi SM, Kohsari I, Teimouri MB, Hajimirsadeghi SS. Thermal behaviour kinetic study of dihydroglyoxime and dichloroglyoxime. Mater Lett. 2007;61:4670–3.
42. Frost RL, Weier ML, Erickson KL. Thermal decomposition of struvite: implications for the decomposition of kidney stones. J Therm Anal Cal. 2004;76:1025–33.
43. Senum GI, Yang RT. Rational approximations of the integral of the arrhenius function. J Therm Anal Cal. 1977;11:445–7.